

## Hydrogenation of titanium-based quasicrystals

A. M. Viano, R. M. Stroud, P. C. Gibbons, A. F. McDowell,  
M. S. Conradi, and K. F. Kelton

*Department of Physics, Washington University, St. Louis, Missouri 63130*

(Received 12 January 1995)

Measurements of hydrogen loading and unloading in a quasicrystal are reported. The icosahedral phase (*i* phase) in a Ti-Zr-Ni alloy demonstrates hydrogen absorption from the gas phase at a temperature of 260 °C and a pressure of 40 atmospheres. The incorporation of hydrogen causes the quasilattice to expand, with an increase in quasilattice constant of almost 7%, from  $a_i = 5.18$  to 5.52 Å. Similar abilities for storing hydrogen are found in high-order crystalline approximant and amorphous phases of like composition. Of the phases examined, the *i* phase absorbs the most hydrogen, giving a hydrogen atom to metal atom ratio ( $[H]/[M]$ ) of 1.6. Initial studies indicate that hydrogen desorption is hindered by phase transitions to stable hydride phases. Hydrogen loading at lower temperatures with higher H<sub>2</sub> pressures favors higher  $[H]/[M]$  ratios for the *i* phase and the crystal approximant, and also minimizes the growth of more stable crystalline hydride phases.

Because of their ability to reversibly absorb significant quantities of hydrogen, crystalline and amorphous transition metals and their alloys have been studied extensively for potential use in hydrogen storage applications. Crystalline Ti and Zr, for example, are capable of storing up to 66 atomic percent (at.%) of hydrogen, corresponding to a hydrogen atom to metal atom ratio ( $[H]/[M]$ ) of 2.<sup>1</sup> Amorphous Zr-Ni is capable of storing hydrogen with an  $[H]/[M]$  of 1.6.<sup>2</sup>

Key factors for determining which materials can store hydrogen include the chemical interactions between metal and hydrogen atoms and the number, type, and size of interstitial sites in the host metal. In most transition metal alloys, the hydrogen prefers to sit in tetrahedrally coordinated sites, making the polytetrahedral Laves phases particularly attractive.<sup>3</sup> The icosahedral phase, the most common quasicrystal phase showing the rotational symmetry of the icosahedral point group, is likely dominated by local tetrahedral order. Surprisingly, hydrogen absorption in *i*-phase materials has received almost no attention. This is probably because most quasicrystals are formed in aluminum alloys, which do not have favorable chemistry for hydrogen storage. Though less well studied, icosahedral quasicrystals are also found frequently in titanium-3*d* transition metal alloys,<sup>4,5</sup> which have favorable chemistry. The dominance of polytetrahedral order and the favorable hydrogen-metal chemistry make these materials potentially useful for hydrogen storage applications, motivating the present study.

Early studies by us<sup>6</sup> and others<sup>7</sup> have demonstrated that Ti-3*d* transition metal-Si icosahedral phases can absorb hydrogen from the gas phase and by electrolytic methods. The amount of hydrogen loaded in these cases, however, was not determined. Further, the influence of surface conditions, the effect of alloy composition, the kinetics of sorption and desorption, and the unloading and cycling characteristics for these materials are as yet unknown. Here, we report the first measurements of hydrogen loading in Ti-Zr-Ni icosahedrally ordered alloys. Constituting the most ordered class of Ti-based quasicrystals, the phases formed in these alloys are known to be extremely sensitive to Si composition. By varying the Si over a range of only 4 at. %, it is possible to go

continuously from the *i* phase to high-order cubic approximants to an icosahedrally ordered metallic glass.<sup>8</sup> As we show here, all of these phases absorb significant amounts of hydrogen (up to  $[H]/[M] = 1.6$  in the *i* phase). In addition to pointing to possible applications, these results open up new windows of investigation into quasicrystal structures. Planned NMR and neutron diffraction studies on hydrogenated and deuterated samples will provide information about the local atomic structure and can probe the dynamics of hydrogen diffusion through a quasilattice.

Alloy ingots prepared by arc melting were crushed and melt-spun to form rapidly quenched ribbons as described elsewhere.<sup>8</sup> The alloy composition was adjusted to give the *i* phase, crystal approximant, or metallic glass on quenching. Three alloys were investigated; Ti<sub>45</sub>Zr<sub>38</sub>Ni<sub>17</sub>, Ti<sub>53</sub>Zr<sub>27</sub>Ni<sub>20</sub>, and Ti<sub>53</sub>Zr<sub>27</sub>Ni<sub>20</sub>(+Si). The rapidly quenched Ti<sub>45</sub>Zr<sub>38</sub>Ni<sub>17</sub> alloy contained only the icosahedral phase. The amorphous Ti<sub>53</sub>Zr<sub>27</sub>Ni<sub>20</sub> alloy contained between 2 and 3 at. % Si, resulting from contamination from the fused silica quenching tube. Si has been found to enhance amorphous phase formation in these alloys.<sup>8</sup> The Ti<sub>53</sub>Zr<sub>27</sub>Ni<sub>20</sub> alloy made with no measurable Si contamination contained a phase mixture of high-order Fibonacci rational approximants, including the 3/2 and the 5/3 cubic approximants.<sup>8</sup>

Samples were investigated with x-ray powder diffraction (XRD) and transmission electron microscopy (TEM). TEM investigations using a JEOL 2000FX equipped with a Noran energy dispersive spectrometer (EDS) were made to obtain local compositional and phase microstructural information. TEM specimens of the as-quenched ribbon were prepared by ion milling, using a liquid nitrogen cooled sample stage to minimize milling-induced artifacts. Samples of the hydrogenated materials were ground into a fine powder for TEM and XRD investigations.

Hydrogenation of the ribbon was carried out in one of two Sieverts'-type systems.<sup>9</sup> Initially, a low-pressure (less than one atmosphere) system was used. In this case, the hydrogenation temperatures were determined simply by heating the sample until surface barriers were overcome and hydrogen absorption occurred, as indicated by a decreasing gas pres-

sure. These temperatures were 350 °C for the *i* phase, 450 °C for the crystal approximant, and 500 °C for the glass. In order to avoid transformations resulting from these high temperatures, a second hydrogenation system was constructed for use with higher hydrogen pressures and lower temperatures. In this case, hydrogenation was carried out at 260 °C and 40 atmospheres. The temperature was chosen to be as low as possible, to avoid crystallization of the metastable *i* phase (which occurs at 650 °C in the absence of hydrogen<sup>8</sup>), while maintaining reasonable kinetics for hydrogen uptake. The hydrogenation time varied from a few minutes in the high-temperature–low-pressure case to 12 h for the low-temperature–high-pressure experiments. Homogeneity of hydrogen concentration was ensured by keeping the samples at the hydrogenation temperature until the pressure had stabilized, signaling that hydrogen uptake had ceased.

During the high-temperature–low-pressure hydrogenation, pieces of ribbon were placed in a quartz tube attached to a liquid nitrogen trapped diffusion-pumped vacuum system, both of known volume. After evacuation, the system was back-filled with less than one atmosphere of hydrogen gas of standard purity. In a volume of 216 cc, pressures ranging from 60 to 242 Torr were used to investigate hydrogen uptake and transformation behaviors. It was found that the starting pressure was not a factor in the induced transformations, as discussed below, but is a possible limitation of the hydrogen uptake. The sample tube was then heated, and the pressure was monitored with an Edwards capacitance manometer, capable of measuring pressures from 0 to 1000 Torr, with a resolution of  $\pm 0.15\%$ . Hydrogen absorption causes a drop in pressure and, after cooling and stabilization, the pressure difference and the known volumes were used to calculate the amount of hydrogen absorbed by the sample.

For the low-temperature–high-pressure hydrogenation, samples were placed in a small chamber in a stainless-steel, copper-gasketed vessel. This was connected to an analog high-pressure gauge, capable of reading pressures between 0 and 3000 psi with a resolution of 50 psi (for details, see Ref. 10). The roughness of this gauge and the possibility of loading more than one sample at a time made the normal volumetric titration method of calculating hydrogen concentration in each sample inapplicable. Each sample was wrapped in aluminum foil to avoid sample loss while allowing exposure to the hydrogen, and weighed before and after hydrogenation on a Cahn electrobalance with an accuracy of  $\pm 5 \mu\text{g}$ . Aluminum foil exposed to H under the same conditions showed no weight increase. Since the hydrogenated ribbons of the *i* phase and the crystal approximants were very brittle, care was required to avoid any loss of the sample during the weighing procedure. The amount of hydrogen absorbed was calculated from the weight increase. The hydrogen concentrations reported here were obtained consistently for several samples hydrogenated under the same conditions. Weight measurements were also used to check the hydrogen content of samples hydrogenated at high temperature and low pressure; agreement with the pressure difference calculations was within 4 at. %.

No treatments were given to the surfaces of the as-quenched ribbons prior to hydrogenation. Though significant quantities of hydrogen were loaded under both high and low pressure, the low-temperature–high-pressure experiments

produced the highest  $[\text{H}]/[M]$  ratios for the *i* phase and crystal approximants, 1.6 and 1.4 respectively.  $[\text{H}]/[M]$  ratios of 1.2, 0.7, and 0.9 were obtained for the *i* phase, the crystal approximant, and the metallic glass respectively under the high-temperature–low-pressure hydrogenation conditions. The hydrogenation conditions were found to be critical for the phase changes and microstructural development, as discussed below.

Powder x-ray diffraction patterns for as-quenched ribbons of the *i* phase ( $\text{Ti}_{45}\text{Zr}_{38}\text{Ni}_{17}$ ) and the crystalline approximants ( $\text{Ti}_{53}\text{Zr}_{27}\text{Ni}_{20}$ ) are shown in Figs. 1(a) and 1(d), respectively. The quasicrystal peaks are indexed following the 6-index method first proposed by Bancel *et al.*<sup>11</sup> Though the approximant phases are crystalline and can be indexed to a large unit-cell cubic phase,<sup>8</sup> the peak positions are so similar to those from the *i* phase that all are indexed as quasicrystalline here to simplify comparison. All visible peaks in the as-quenched materials index to the *i* phase or the approximant, with the exception of a small unidentified peak between the (100000) and the (110000) peaks.

The x-ray diffraction data following low-temperature–high-pressure and high-temperature–low-pressure hydrogenation are compared with those of the as-quenched ribbons in Fig. 1. The *i* phase is retained after hydrogenation at low temperature (260 °C) [Fig. 1(b)], while it has completely transformed to a mixture of crystalline hydride phases after hydrogenation at 350 °C [Fig. 1(c)]. Similar features are reflected in the x-ray patterns from the crystal approximants [Figs. 1(d)–1(f)]. The phase transitions accompanying hydrogenation presumably result from the difference in hydrogenation temperatures. Differential scanning calorimetry of as-quenched ribbons of  $\text{Ti}_{45}\text{Zr}_{38}\text{Ni}_{17}$  indicates that the *i* phase is quite stable, not transforming at a significant rate until the temperature is increased above 650 °C. That the hydrogenated *i* phase transforms here at much lower temperatures indicates that the hydrogen enhances the transformation. Whether this represents a thermodynamic change in stability or an enhanced atomic mobility is not yet known.

A comparison of Figs. 1(a) and 1(b) or 1(d) and 1(e) showing the results of the low-temperature–high-pressure hydrogenation indicates that the hydrogen introduces a significant strain in the lattice and quasilattice, broadening the x-ray peaks and shifting them to lower angle. The small amount of broadening compared to the shift in angle indicates homogeneous hydrogen loading. For the *i* phase, the peak shift corresponds to a 6.6% increase in the average quasilattice parameter, from  $a_i = 5.18 \text{ \AA}$  for the as-quenched alloy to  $a_i = 5.52 \text{ \AA}$  in the hydrogenated sample. The small peaks not initially present in the as-quenched *i*-phase pattern indicate some phase transformation even at 260 °C. TEM studies of the hydrogenated material indicate that the new phase forms as nanometer-sized precipitates within the *i*-phase grains. Based on the intensities of the x-ray peaks, these precipitates constitute approximately 10% of the sample. EDS measurements indicate that these are similar in composition to the hydrogenated quasicrystal. Though structural studies were hampered by their small size, making tilting experiments difficult, the precipitates are most likely the  $\text{MgZn}_2$  structure, an hcp Laves phase dominated by tetrahedral packing. Semenenko *et al.*<sup>9</sup> have shown that  $\text{TiZrNiH}_{3.7}$  ( $[\text{H}]/[M] = 1.23$ ) has this structure, with

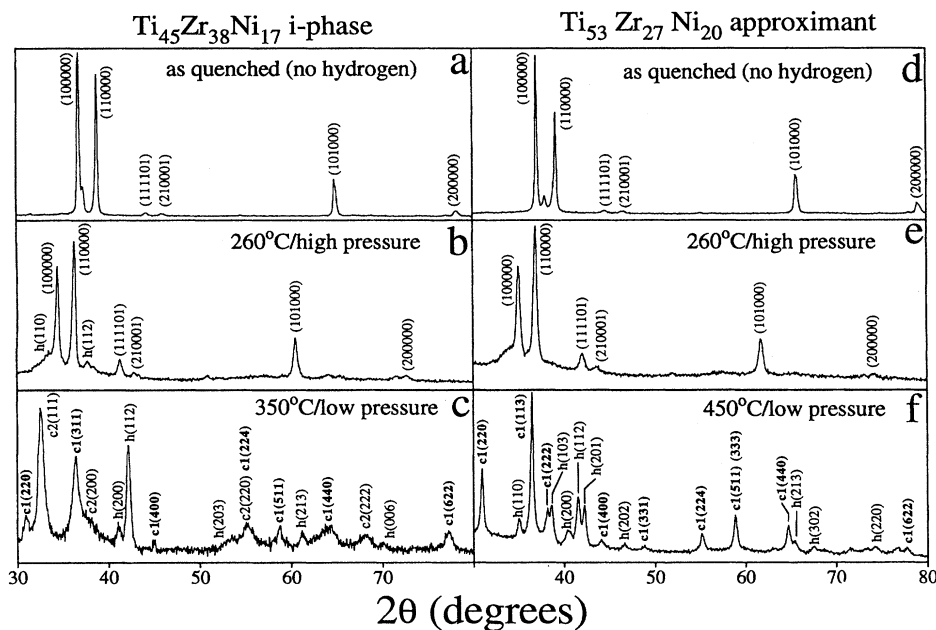


FIG. 1. X-ray diffraction patterns for the as-quenched and hydrogenated materials. The diffracted intensity (arbitrary units) is plotted as a function of  $2\theta$ . Panels a–c refer to the  $\text{Ti}_{45}\text{Zr}_{38}\text{Ni}_{17}$  alloy (as-quenched *i* phase); panels d–f are for the  $\text{Ti}_{53}\text{Zr}_{27}\text{Ni}_{20}$  alloy (as-quenched crystal approximant). Both the *i* phase and crystalline approximant peaks are indexed with the 6-index method proposed by Bancel *et al.*<sup>11</sup> For the crystalline phases, *h* represents the hcp Laves phase, *c1* the large fcc Laves phase, and *c2* the small fcc  $\text{ZrH}_2$ . Hydrogenation temperature and pressure conditions are indicated in each case.

$a = 5.56 \text{ \AA}$  and  $c = 9.01 \text{ \AA}$ . Further, our annealing studies have shown that the nonhydrogenated  $\text{Ti}_{53}\text{Zr}_{27}\text{Ni}_{20}$  *i* phase crystallizes to the  $\text{MgZn}_2$  phase with  $a = 5.21 \pm 0.04 \text{ \AA}$  and  $c = 8.53 \pm 0.04 \text{ \AA}$ . Indexing the small peaks in the x-ray pattern of the low-temperature–high-pressure hydrogenated *i* phase (panel b) to this structure gives  $a = 5.60 \pm 0.04 \text{ \AA}$  and  $c = 9.47 \pm 0.04 \text{ \AA}$ . That these values are larger than those found in the nonhydrogenated annealed *i* phase and those reported by Semenenko *et al.* suggests that the  $\text{MgZn}_2$  phase obtained here has an  $[\text{H}]/[\text{M}]$  ratio higher than 1.23. The larger expansion along the *c* direction hints that the additional H sites lie in that direction. This increase in lattice parameter may also be a result of the higher Zr concentration in the hydrogenated  $\text{Ti}_{45}\text{Zr}_{38}\text{Ni}_{17}$ , as compared to our nonhydrogenated *i* phase and the material of Semenenko *et al.*

TEM studies confirm the x-ray results showing that hydrogenation at high temperature and low pressure transforms the *i* phase to an extremely fine microstructure of different crystalline phases [Figs. 1(a) and 1(c)]. EDS studies show that the compositions of the 10–20 nm sized grains varied. Some were extremely Zr or Ti rich, while others had compositions similar to the hydrogenated *i*-phase grains resulting from the high-pressure loading. The x-ray pattern can be indexed to a mixture of three phases:  $\text{MgZn}_2$  hcp Laves phase with  $a = 5.10 \pm 0.04 \text{ \AA}$  and  $c = 8.07 \pm 0.04 \text{ \AA}$ , an fcc phase with  $a_0 = 8.16 \pm 0.08 \text{ \AA}$ , and another fcc phase with  $a_0 = 4.77 \pm 0.05 \text{ \AA}$ . The 8.16  $\text{\AA}$  fcc phase is likely  $\text{Ti}_2\text{ZrH}_4$ , which has a reported  $a_0 = 8.19 \text{ \AA}$  (fcc)  $\text{MgCu}_2$ -type Laves structure.<sup>12</sup> This matches well with the Ti-rich grains. The small fcc phase can be identified as fcc  $\text{ZrH}_2$  with a reported lattice constant of 4.76  $\text{\AA}$ ,<sup>13</sup> and corresponds to the Zr-rich grains. Interestingly, the lattice param-

eters in the  $\text{MgZn}_2$ -type phase in this hydrogenated material are less than those of our nonhydrogenated samples ( $a = 5.21 \text{ \AA}$ ,  $c = 8.53 \text{ \AA}$ ), while the lattice parameters of the  $\text{MgZn}_2$  phase in the low-temperature–high-pressure hydrogenated material are larger ( $a = 5.60 \text{ \AA}$  and  $c = 9.47 \text{ \AA}$ ). Evidently the lattice parameters are sensitive to both the metal composition and the hydrogen concentration. Just as  $\text{TiZrNiH}_{3.7}$  liberates hydrogen readily at temperatures above 200  $^\circ\text{C}$ ,<sup>12</sup> the higher temperatures of our lower-pressure loading (350  $^\circ\text{C}$ ) may have inhibited the hydrogenation of the  $\text{MgZn}_2$ -type phase. Since the  $\text{ZrH}_2$  phase is present only after this higher-temperature loading, the mobile hydrogen might have been instrumental in  $\text{ZrH}_2$  formation.

Like the *i* phase, the crystal approximants also experience an increase in lattice parameter upon hydrogenation, increasing the effective quasilattice constant from 5.13 to 5.43  $\text{\AA}$  [compare Figs. 1(d) and 1(e)]. This sample also contained 20–50 nm grains that were rich in Ti. Selected area diffraction studies showed this to be fcc with  $a_0 = 4.25 \pm 0.05 \text{ \AA}$ . Within the limits imposed by the electron microscope, and with the substitutional introduction of some smaller Ni atoms, this Ti-rich phase might be fcc  $\text{TiH}_2$ , for which  $a_0 = 4.40 \text{ \AA}$ .<sup>13</sup> Again like the *i* phase, the approximants were transformed upon loading at a higher temperature and lower pressure to a phase mixture of an  $8.16 \pm 0.07 \text{ \AA}$  fcc phase, corresponding to  $\text{Ti}_2\text{ZrH}_4$ , and the  $\text{MgZn}_2$  hexagonal Laves phase with  $a = 5.11 \pm 0.04 \text{ \AA}$  and  $c = 8.16 \pm 0.04 \text{ \AA}$ . The  $\text{Ti}_2\text{ZrH}_4$  phase constitutes the largest volume fraction of the sample, and there is no  $\text{ZrH}_2$  in this case.

Hydrogenation of the amorphous samples was successful at high temperatures and low pressures only. The failure of

low-temperature-high-pressure (260 °C/40 atm) experiments may indicate a higher surface barrier to hydrogen absorption in the glass. A temperature of 500 °C was required for hydrogenation at low pressure, approximately 150 °C higher than for the *i* phase, supporting this hypothesis. X-ray patterns taken from the now brittle hydrogenated glass confirmed that it remained amorphous, with a 5.5% increase in the *d* spacing corresponding to the first peak in the structure factor, again indicating that the incorporation of the hydrogen caused an expansion of the structure.

Hydrogen desorption was attempted for the *i* phase and crystal approximant (both hydrogenated at 260 °C and 40 atm) by heating the samples in an evacuated vessel of known volume and monitoring the pressure with a capacitance manometer. A pressure versus temperature curve for  $0 < T < 650$  °C shows several plateau regions, corresponding to several phase transitions. After heating to 650 °C, only 10% of the hydrogen has evolved from the sample. The x-ray diffraction pattern and the phases present are identical to those of the sample hydrogenated at a high temperature and low pressure [Fig. 1(c)]. No *i* phase remains. The sample consists of 10–20 nm grains of fcc ZrH<sub>2</sub> ( $a_0 = 4.75 \pm 0.03$  Å), hexagonal TiZrNiH<sub>3.7</sub> ( $a = 5.08 \pm 0.04$  Å and  $c = 8.04 \pm 0.04$  Å), and fcc Ti<sub>2</sub>ZrH<sub>4</sub> ( $a_0 = 8.17 \pm 0.05$  Å). The x-ray diffraction pattern of an *i*-phase sample heated to 530 °C (in the first plateau region) shows an approximately equal mixture of the *i* phase and ZrH<sub>2</sub>. A decreased quasilattice constant ( $a_i = 5.45$  Å, down from the hydrogenated value of 5.52 Å) indicates a loss in hydrogen from the *i* phase. However, the increase in pressure due to hydrogen evolution was minimal, corresponding to only 10% of the amount absorbed. This suggests that instead of being liberated from the sample, the hydrogen is involved in the phase transformations, leaving the *i* phase but being quickly absorbed by the growing crystalline phases. These desorption studies show the role of *high temperatures* in transforming the *i* phase during hydrogenation, as opposed to lower H<sub>2</sub> pressure.

Though calorimetric studies of the as-quenched *i* phase and approximants in an inert atmosphere show that they are stable to 650 °C,<sup>8</sup> it is clear that the presence of hydrogen lowers the transition temperatures significantly, likely stabilizing the crystalline hydride phases. This is similar to the many examples of hydrogen-driven phase transitions in crystalline metal hydride systems.<sup>1</sup>

We have demonstrated that titanium-based quasicrystals can absorb significant quantities of hydrogen, up to  $[H]/[M] = 1.6$  in Ti<sub>45</sub>Zr<sub>38</sub>Ni<sub>17</sub>, resulting in a large expansion of the quasilattice. The large hydrogen uptake ( $[H]/[M] = 1.6$ ) reflects the favorable chemistry and presumed large number of tetrahedral sites. Lower-temperature-high-pressure hydrogenation inhibits the transformation of the *i* phase to more stable crystalline hydride phases. In the *i*-phase alloy studied, liberation of the stored hydrogen was hampered by the formation of crystalline hydride phases at temperatures above 500 °C. Problems with both absorption and desorption may be lessened by changes in the alloy composition and by surface treatments,<sup>1</sup> possibly allowing for further reductions in the temperature required for hydrogenation.

Aside from the possible technological applications, these results provide a new tool for examining the quasicrystal structures and for exploring diffusion in a quasilattice. Planned neutron diffraction and nuclear magnetic resonance studies of hydrogenated and deuterated samples of the *i* phase and related crystalline and amorphous phases will allow determinations of the local site symmetries and chemical environments. Further, by loading the quasicrystals to different degrees, the phase transitions due to hydrogen residing in the interstices of a quasilattice can be studied for the first time.

The authors gratefully acknowledge support from NSF grants DMR92-03052 and DMR94-03667. We thank D. T. Peterson and D. R. Torgeson of Iowa State University and W. B. Yelon of the University of Missouri for helpful comments during the early stages of this work.

<sup>1</sup>W. M. Mueller, J. P. Blackledge, and G. G. Libowitz, *Metal Hydrides* (Academic, New York, 1968).

<sup>2</sup>R. Kirchheim, F. Sommer, and G. Schluckerbier, *Acta Metall.* **30**, 1059 (1982).

<sup>3</sup>J. H. Harris, W. A. Curtin, and M. A. Tenhover, *Phys. Rev. B* **36**, 5784 (1987).

<sup>4</sup>C. Dong, Z. K. Hei, L. B. Wang, Q. H. Song, Y. K. Wu, and K. H. Kuo, *Scr. Metall.* **20**, 1155 (1986).

<sup>5</sup>K. F. Kelton, *Int. Mat. Rev.* **38**, 105 (1993).

<sup>6</sup>A. M. Viano, P. C. Gibbons, and K. F. Kelton, *Bull. Am. Phys. Soc.* **38**, 681 (1993).

<sup>7</sup>D. Bahadur, V. Srinivas, and R. A. Dunlap, *J. Non-Cryst. Solids* **109**, 54 (1989).

<sup>8</sup>X. Zhang, R. M. Stroud, J. L. Libbert, and K. F. Kelton, *Philos. Mag. B* **70**, 927 (1994).

<sup>9</sup>K. N. Semenenko, V. N. Verbetskii, S. V. Mitrokhin, and V. V. Burnasheva, *Russ. J. Inorg. Chem. (English translation)* **25**, 1731 (1980).

<sup>10</sup>A. F. McDowell, Ph.D. thesis, Cornell University, 1993 (unpublished).

<sup>11</sup>P. A. Bancel, P. A. Heiney, P. W. Stephens, A. I. Goldman, and P. M. Horn, *Phys. Rev. Lett.* **54**, 2422 (1985).

<sup>12</sup>N. F. Miron, V. I. Shcherbak, V. N. Bykov, and V. A. Levdik, *Sov. Phys. Crystallogr.* **16**, 266 (1971).

<sup>13</sup>P. Villars and L. D. Calvert, *Pearson's Handbook of Crystallographic Data* (American Society for Metals, Metals Park, OH, 1985).